Journal of Ceramic Processing Research. Vol. 14, No. 1, pp. 8~11 (2013)

J O U R N A L O F
Ceramic Processing Research

Surface, structural, and optical property variations of ZnO nanocrystals formed on Si substrates due to thermal treatment

Young Soo No, Su Youn Kim and Tae Whan Kim*

National Research Laboratory for Nano Quantum Electronics Devices, Department of Electronics and Computer Engineering, Hanyang University, Seoul 133-791, Korea

ZnO nanocrystals were formed on Si substrates using spin coating and thermal annealing. X-ray diffraction patterns showed that the intensity of the ZnO (0002) peak corresponding to the ZnO [0001] nanocrystals increased with an increase in annealing temperature up to 700 °C, indicative of the improvement of the crystallinity of the ZnO nanocrystals. The photoluminescence spectra at 13 K for ZnO nanocrystals formed on the Si substrates showed that the strong exciton peak related to the near-band-edge emission was shifted to a lower energy with increasing annealing temperature resulting from the increase in the size of the ZnO nanocrystals.

Key words: Thermal annealing, ZnO nanocrystal, Surface property, Structural property, Optical property.

Introduction

Nanocrystals based on wide-band-gap compound semiconductors have currently been receiving considerable attention because of their potential applications in electronic and optoelectronic devices operating at lower currents and higher temperatures [1-5]. Among the various types of nanocrystals, because ZnO nanocrystals are wide-band-gap semiconductors with superior physical properties of large exciton binding energies and excellent chemical stabilities [6, 7], they are particularly interesting due to their potential applications in optoelectronic devices, such as light-emitting diodes [8], laser diodes [9], and solar cells [10]. In particular, ultraviolet lasers fabricated utilizing ZnO materials operating at room temperature have emerged as excellent candidates for potential applications in next-generation promising optoelectronic devices [11-13]. Even though some studies concerning the formation and the physical properties of ZnO nanocrystals on various substrates have been reported [14-18], almost all of the reported materials have been formed by molecular beam epitaxy, metal-organic chemical vapor deposition, pulsed laser deposition, and sputtering methods. ZnO/Si hetero-structures, which are fabricated by utilizing the combined advantages of the large excitonic binding energy of a ZnO thin film and cheap Si substrates, have been particularly interesting due to their promising applications for optoelectronic devices operating in the blue region of the spectrum [19]. Even though some studies on the formation and the physical properties of ZnO nanocrystals via a simple method have been performed [19-21], very few studies concerning the effects of thermal annealing on the surface, the structural, and the optical properties of ZnO nanocrystals formed on Si (100) substrates have been conducted. Furthermore, systematic studies concerning the effects of thermal annealing on the surface, the structural, and the optical properties of ZnO nanocrystals formed on Si (100) substrates are very important for enhancing the efficiency of optoelectronic devices based on ZnO nanocrystals.

This paper reports data for the effects of thermal annealing on the surface, the structural, and the optical properties of ZnO nanocrystals formed on p-Si (100) substrates by using a spin-coating method. Atomic force microscopy (AFM) and X-ray diffraction (XRD) measurements were carried out to investigate the surface and the structural properties of the annealed ZnO nanocrystals. Photoluminescence (PL) measurements were performed to investigate the optical properties of the annealed ZnO nanocrystals.

Experimental Details

The samples used in this study were formed on p-Si (100) substrates by using a spin-coating method. The carrier concentration of the B-doped p-Si substrates with a (100) orientation used in this experiment was 1×10^{15} cm^{-3}. The zinc acetate dihydrate was used as a starting material, and the methanol solution was used as a solvent [22]. After the zinc acetate dihydrate was dissolved in the methanol solution at room temperature, the saturated solution was stirred at 60 °C for 2 h to obtain a uniform solution. The prepared solution was dropped onto the Si substrates, as shown in Fig. 1(a),

*Corresponding author:
Tel : +82-2-2220-0354
Fax: +82-2-2292-4135
E-mail: twk@hanyang.ac.kr

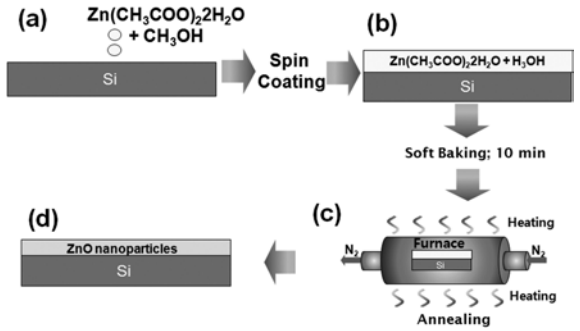

Fig. 1. Schematic diagrams of the formation processes of the ZnO nanocrystals on the Si (100) substrates.

and then rotated by a spin coater at 7000 rpm for 30 s. After the zinc acetate dihydrate was deposited by spin coating, as shown in Fig. 1(b), the samples were dried on a hotplate for 10 minutes in order to remove the solvent and organic residuals. The samples were annealed in an air atmosphere at 300, 500, 700, and 900 °C for 2 h, as shown in Fig. 1(c). ZnO nanocrystals were formed by thermal treatment resulting from the vaporization of the acetate acid, as shown in Fig. 1(d). The schematic diagrams of the formation processes of the ZnO nanocrystals on the Si (100) substrates are shown in Fig. 1. The size of the ZnO nanocrystals can be controlled by changing the annealing temperature and time.

The AFM measurements were performed using a Digital Instrument Dimension TM 3100 (Veeco). The XRD measurements were performed using a Rigaku D/MAX-B diffractometer with Cu K_α radiation. The PL measurements were carried out using a 50 cm monochromator equipped with an RCA 31034 photomultiplier tube. The excitation source was the 3250 Å line of a He-Cd laser, and the sample temperature was kept at 13 K by using a He displex system.

Results and Discussion

Figure 2 shows that AFM images of ZnO nanocrystals formed on the Si substrates annealed at (a) 300, (b) 500, (c) 700 and (d) 900 °C. The sizes of the ZnO nanocrystals formed on the Si substrates annealed at 300, 500, 700 and 900 °C, as determined from the AFM measurements, are 3.71, 16.14, 21.22, and 38.69 nm, respectively, as shown in Fig. 2. AFM images show that the size of the ZnO nanocrystals increases with increasing annealing temperature. The increase in the size of the ZnO nanocrystals with an increase in the annealing temperature is attributed to the coalescence of nanocrystals due to the higher thermal energy. However, when the annealing temperature is above 900 °C, the ZnO nanocrystals transform into ZnO agglomerates due to the continuous additional coalescence.

Figure 3 shows XRD patterns for the ZnO nanocrystals on the Si substrates annealed at (a) 300, (b) 500, (c) 700 and (d) 900 °C. The (0002) $K_{\alpha 1}$ diffraction peaks

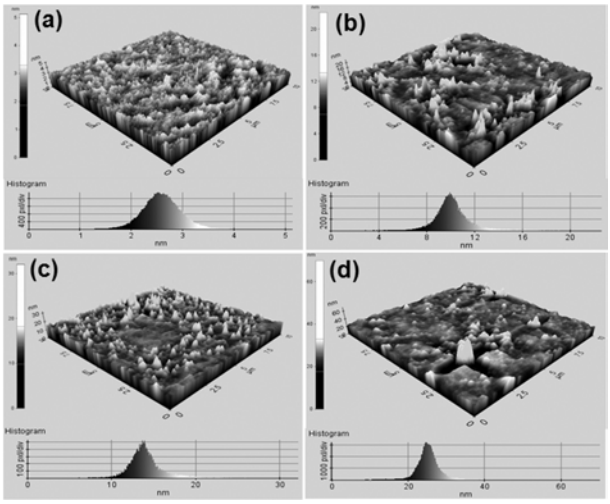

Fig. 2. Atomic force microscopy images of ZnO nanocrystals formed on the Si substrates annealed at (a) 300, (b) 500, (c) 700 and (d) 900 °C. The scanning area of the surface is 10 × 10 μm^2.

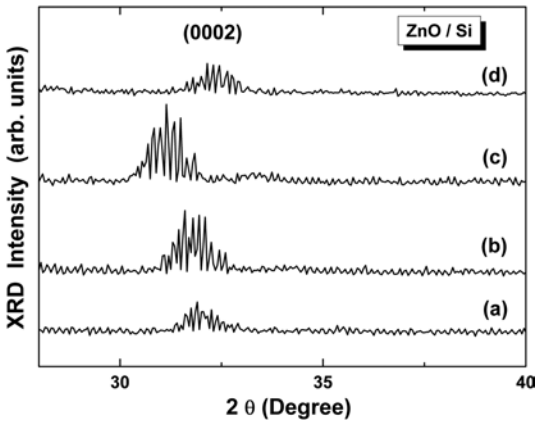

Fig. 3. X-ray diffraction patterns of the ZnO nanocrystals formed on the Si (100) substrates annealed at (a) 300, (b) 500, (c) 700 and (d) 900 °C.

corresponding to the ZnO (0001) films annealed at 300, 500, 700 and 900 °C are clearly observed in Fig. 3 [23]. The XRD patterns indicate that the annealed ZnO nanocrystals have a strong c-axis orientation, this orientation giving the lowest surface free energy [24]. The intensity of the XRD pattern corresponding to the ZnO (0002) peak for the ZnO/Si heterostructure increases with increasing annealing temperature up to 700 °C, and the full width at half-maximum for the (0002) diffraction peak for the ZnO nanocrystals decreases, indicative of an increase in the grain size and a strongly preferential orientation of the (0001) hexagonal structure due to an increase in the annealing temperature up to 700 °C. When the annealing temperature is increased to 800 °C, the XRD intensity for the (0002) diffraction peak for the ZnO nanocrystals decreases resulting from an increase in the density of the dislocations. When the ZnO/Si samples are annealed in an air atmosphere, the ZnO nanocrystals might be significantly affected due to the large thermal expansion between the ZnO nanocrystals and the Si

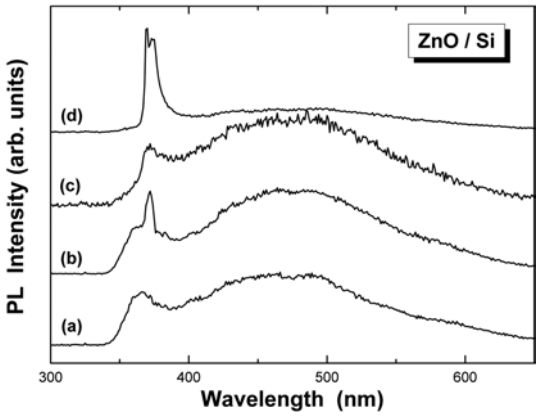

Fig. 4. Photoluminescence spectra at 13 K of the ZnO nanocrystals formed on the Si substrate annealed at (a) 300, (b) 500, (c) 700 and (d) 900 °C.

substrate [25], resulting in the improvement of the crystallinity of the ZnO nanocrystals.

Figure 4 shows that PL spectra at 13 K for the ZnO nanocrystals formed on the Si substrates annealed at 300, 500, 700 and 900 °C. The excitonic peaks were shifted to higher energy with a decrease in the annealing temperature due to quantum-confinement effect resulting from a decrease in the size of the ZnO nanocrystals and to the relaxation of stress for the ZnO nanocrystals. The peak at 365 nm for the ZnO nanocrystals formed on the Si substrates annealed at 300 °C is attributed to the near band-edge (NBE) emissions of the excitons bound to donors (DX), as shown in Fig. 4(a). The emission peak at 370 nm for the ZnO/Si hetero-structures annealed at 900 °C, which is lower than the band edge emission of the bulk ZnO materials, is attributed to the NBE emissions of the excitons bound to acceptors (AX) [26]. The PL spectrum for the ZnO nanocrystals formed on Si substrates annealed at 900 °C shows only strong exciton peaks related to the NBE emissions without exhibiting a green-emission peak. The DX and AX emission peaks at 370 nm and 375 nm shift to high energy sides of 365 nm and 372 nm, respectively, with a decrease in the annealing temperature from 900 to 300 °C due to quantum confinement effect resulting from the decrease in the size of the ZnO nanocrystals. The PL peak around 450 nm for ZnO nanocrystals formed on p-Si (100) substrates is related to the deep-level (DL) emission, and the DL emission might be attributed to oxygen vacancies or zinc interstitials [27]. The PL intensity corresponding to the DL emission significantly decreases with increasing annealing temperature.

Summary and Conclusions

The effects of thermal annealing on the surface, the structural, and the optical properties of ZnO nanocrystals on Si substrates using spin coating were investigated. AFM and XRD results showed that the ZnO nanocrystals with a c-axis preferential orientation in the [0001] crystal direction were formed on Si (100) substrates. AFM images showed that the size of ZnO nanocrystals increased with an increase in the annealing temperature. XRD patterns showed that the (0002) peak intensity corresponding to the ZnO nanocrystals increased with an increase in the annealing temperature up to 700 °C, indicative of the improvement of the crystallinity of the ZnO nanocrystals. The PL spectra at 13 K for ZnO nanocrystals on Si substrates showed that the strong exciton peak related to the NBE emission was shifted to a lower energy with an increase in the annealing in the temperature resulting from the increase in the size of the ZnO nanocrystals.

Acknowledgment

The author would like to appreciate the financial support by the Converging Research Center Program through the National Research foundation of Korea (NRF) funded by the Ministry of Education, Science and Technology (grant number 2012K001286). This work was supported by Leading Foreign Research Institute Recruiment Program through the National Research Foundation of Korea (NRF) funded by the Ministry of Education, Science and Technology (MEST) (No. 2012-00109).

References

1. M. Achermann, M.A. Petruska, S. Kos, D.L. Smith, D.D. Koleske, V.I. Klimov, Nature 429 (2004) 642-646.
2. T.W. Kim, J.W. Shin, J.Y. Lee, J.H. Jung, J.W. Lee, W.K. Choi, S. Jin, Appl. Phys. Lett. 90 (2007) 051915-1-051915-3.
3. R.J. Warburton, C. Schaflein, D. Haft, F. Bickel, A. Lorke, K. Karrai, J.M. Garcia, W. Schoenfeld, P.M. Petroff, Nature 405 (2000) 926-929.
4. X. Li, Y. Wu, D. Steel, D. Gammon, T.H. Stievater, D.S. Katzer, D. Park, C. Piemarocchi, L.J. Sham, Science 301 (2003) 809-811.
5. N.J. Craig, J.M. Taylor, E.A. Lester, C.M. Marcus, M.P. Hanson, A.C. Gossard, Science 304 (2004) 565-567.
6. T. Aoki, Y. Hatanaka, D.C. Look, Appl. Phys. Lett. 76 (2000) 3257-3258.
7. R.F. Service, Science 276 (1997) 895-895.
8. W.Z. Xu, Z.Z. Ye, Y.J. Zeng, L.P. Zhu, B.H. Zhao, L. Jiang, J.G. Lu, H.P. He, S.B. Zhang, Appl. Phys. Lett. 88 (2006) 173506-1-173506-3.
9. H. Kim, C.M. Gilmore, J.S. Jorwitz, A. Pigue, H. Murafa, G.P. Kushto, R. Schlaf, Z.H. Kafafi, D.B. Chrisey, Appl. Phys. Lett. 76 (2000) 259-261.
10. U. Rau, M. Schmidt, Thin Solid Films 387 (2001) 141-146.
11. Z.K. Tang, G.K. L. Wong, P. Tu, M. Kawasaki, A. Ohtomo, H. Koinuma, Y. Segawa, Appl. Phys. Lett. 72 (1998) 3270-3272.
12. S.F. Yu, C. Yuen, S.P. Lau, H.W. Lee, Appl. Phys. Lett. 84 (2004) 3244-3246.
13. H.D. Li, S.F. Yu, A.P. Abiyasa, C. Yuen, S.P. Lau, H.Y. Yang, E.S.P. Leong, Appl. Phys. Lett. 86 (2005) 261111-1-

261111-3.
14. A. Mitra, R.K. Thareja, J. Appl. Phys. 89 (2001) 2025-2028.
15. Z. Wang, H. Zhang, L. Zhang, J. Yuan, S. Yan, C. Wang, Nanotechnology 14 (2003) 11-15.
16. Z.L. Wang, J. Phys.-Condes. Matter 16 (2004) R829-R858.
17. W.J.E. Beek, M.M. Wienk, M. Kemerink, X. Yang, R.A.J. Janssen, J. Phys. Chem. B 109 (2005) 9505-9516.
18. W.M. Hlaing Oo, M.D. McCluskey, A.D. Lalonde, M.G. Norton, Appl. Phys. Lett. 86 (2005) 073111-1-073111-3.
19. Y. Sun, J.B. Ketterson, G.K.L. Wong, Appl. Phys. Lett. 77 (2000) 2322-2324.
20. R.D. Yang, S. Tripathy, Y. Li, H.-J. Sue, Chem. Phys. Lett. 411 (2005) 150-154.
21. A. Stassinopoulos, R.N. Das, E.P. Giannels, S.H. Anastasiadis, D. Anglos, Appl. Surf. Sci. 247 (2005) 18-24.
22. S.P. Anthony, J.I. Lee, J.K. Kim, Appl. Phys. Lett. 90 (2007) 103107-1-103107-3.
23. N. Fujimure, T. Nishhara, S. Goto, J. Xu, T. Ito, J. Cryst. Growth 130 (1993) 269-279.
24. Y.H. Tong, Y.C. Liu, C.L. Shao, R.X. Mu, Appl. Phys. Lett. 88 (2006) 123111-1-123111-3.
25. Y.J. Li, R. Duan, P.B. Shi, G.G. Qin, J. Cryst. Growth 260 (2004) 309-315.
26. K. Giannakopoulos, N. Boukos, A. Travlos, T. Monteiro, M.J. Soares, M. Peres, A. Neves, M.C. Carmo, Appl. Phys. A: Mat. Sci. & Processing 88 (2007) 41-44.
27. F.K. Shen, G.X. Liu, W.J. Lee, G.H. Lee, I.S. Kim, B.C. Shin, Appl. Phys. Lett. 86 (2005) 221910-1-221910-3.